

Influence on Key Properties of Mn^{2+} Doping in L-ornithine Monohydrochloride Single Crystals: A Non-Linear Optical Material

Shish Pal Rathee^{a,*}, Dharamvir Singh Ahlawat^b & S SHooda^a

^aDepartment of Physics, A I Jat H M College, Rohtak 124 001, India

^bDepartment of Physics, Chaudhary Devi Lal University, Sirsa 125 055, India

Received: 9 Sept 2024; accepted: 4 July 2025

Pure and 1 mol%, 2 mol %, 5 mol% Mn^{2+} doped single crystals of L-ornithine monohydrochloride (LOMHCl) were successfully grown by conventional slow evaporation solution technique (SEST). Effect on crystalline perfection, thermal and mechanical stability and second harmonic generation efficiency on title compound has been explored in detail. Using the Powder X-ray diffraction (XRD) curve, the value of mechanical strain for 1 mol %, 2 mol % and 5 mol % doped crystals were calculated by W-H analysis and found 2.95×10^{-3} , 1.64×10^{-3} and 9.79×10^{-4} respectively. The crystalline perfection in pure as well as in doped crystals was assessed by high-resolution XRD, which results in better crystalline perfection at small and modest level doping concentration. The thermal and mechanical behavior have also been investigated which reveals that incorporated dopant concentration increases both features of the grown crystals. Hardness no. is calculated from hardness curve and is found 1.06, 1.04, 1.04 and 1.03 for undoped and Mn^{2+} doped LOMHCl single crystals respectively. Effect of doping on the second harmonic generation (SHG) efficiency reveals the considerable enhancement and better correlation with the crystalline perfection.

Keywords: Doping, Slow evaporation solution technique, High-resolution X-ray diffraction, Optical transmission, Second harmonic generation efficiency

1 Introduction

In the contemporary world of information technology which includes photonic, opto-electronic and electro-optic devices has galvanized the scientists and technologist for search of some new and promising materials with enhanced optical properties. For the use in non-linear optical applications, a crystal must be able to change the frequency or phase of incident of the laser light passing through it. The crystals possessing not only high second harmonic generation efficiency (SHG) and laser damage threshold (LDT) but should also have good mechanical and thermal stability with better optical transparency are highly preferred¹⁻⁴. Organic materials have large SHG but very less mechanical and thermal stability. In previous studies, it has noted that inclusion of dopants impurities in the crystals results in redistribution of electronic charge. This redistribution can alter the electric-dipole effect in the energy matter interaction, thus rendering the crystal suitable for SHG applications⁵⁻⁷. Some researchers have reported that Cu^{2+} and Fe^{2+} ion can be incorporated in L-Alanine and explained that

transition metal ion manipulate optical transparency in the amino acids in UV region by changing dipole allowed transition^{8, 9}. The doping of Mn^{2+} enhances the NLO properties of crystal and increase the data capability^{10,11}. It becomes much more important to assess the crystalline perfection in the advance technology which includes the single crystal based devices. High-resolution X-ray diffractometry is one of the most useful and efficient technique for the assessment of crystalline perfection and crystal defects^{11, 12}. With the doping of transition metal ion there is not only seen change in physical properties but also found significant enhancement in crystalline perfection which can be examined with the help of HRXRD¹⁰. Influence of Mn^{2+} doping in properties of L-alanine has been studied and successfully correlated with the crystalline perfection¹¹. To the best of my knowledge a few published literature¹² is available on the doping effect of $MnCl_2$ on L-ornithine monohydrochloride crystal

In the present course of work, we have chosen $MnCl_2$ as a potential dopant¹³ and reported first time the influence of Mn^{2+} doping on crystalline perfection, SHG of LOMHCl crystal and a systematic correlation between them at various doping concentration. Impact

*Corresponding author: E-mail: sprathee.jcr@gmail.com

on mechanical and thermal stability of LOMHCl was also successfully carried out which found in well agreement with literature¹².

2 Crystal Growth

The commercially available CDH make AR grade salt of LOMHCl (with 99 % purity) was used after repeated re-crystallization to grow single crystals of pure and doped LOMHCl by most convenient slow evaporation solution technique (SEST). However, the crystal can also be grown by some other method such as slow cooling method, Shankaranayanan-Ramasamy method depending upon the requirement of crystal size and properties, Then $MnCl_2$ of CDH make (with 99% purity) was doped in different concentrations of 1 mol %, 2 mol % and 5 mol % by adding the calculated amount of dopant in the host crystal. The presence of additive in very small amount can influence the crystallization kinetics to a large extent. An additive or a dopant may affect both the activities of crystallizing solute in saturated solution and affect the crystal growth process due to absorption on the growing surface. An important application to this effect of various concentration of doping on the crystal growth process for crystal structure can be used in designing the crystalline drugs with the physiochemical properties.

The calculated amount of $MnCl_2$ is added to the saturated solution of LOMHCl kept in different beakers marked as 1 mol%, 2 mol % and 5 mol % respectively. These solutions were stirred with the help of a magnet stirrer for a period of 8 hours so that homogenous and saturated solutions were prepared. The solutions were filtered through small pours whattman filter paper and kept in well cleaned beakers. These beakers were roofed with a plastic sheet having many pin holes on it and placed undisturbed at room temperature i.e. 35°C. Crystals were harvested in a span of 22-25 days as shown in Fig. 1.

The LOMHCl is a α -amino acid with one carboxylic group ($-COO^-$) as an acceptor and (NH_3^+) as a proton donor group. It crystallizes in the monoclinic crystal

system and $P12_11$ space group. Doping of Mn^{2+} has no significant influence on the crystal structure and structural morphology of the in situ grown crystal.

3 Characterization Techniques

The crystals were initially ground into a fine powder using an agate mortar. To examine alterations in lattice parameters, doped specimens were analyzed by powder XRD analysis employing a Bruker D8 Advanced spectrometer with $CuK\alpha$ radiation. Scans were conducted from 10° to 80° at a rate of $0.001^\circ/s$ at room temperature, ensuring uniform experimental conditions for each specimen along similar planes. To assess the impact of doping on the non-linear efficiency (SHG) of LOMHCl crystals, specimens were undergone the Kurtz powder test. Following crushing and sieving to create a homogeneous powder, the samples were filled into glass capillaries and subjected to Nd: laser excitation at the IISc, Bangalore. The resulting SHG radiations were measured at a wavelength of 532 nm using a photomultiplier tube, with consistent experimental conditions maintained throughout. Additionally, the crystalline perfection of doped crystals was evaluated using HRXRD. A PANalytical multi-crystal X-ray diffractometer, equipped with a fine-focus x-ray source and a Philips X-ray generator, facilitated rocking curve recordings. The specimen underwent rotation about a vertical axis perpendicular to the diffraction plane, and rocking curves were recorded across the diagonal of the sample after lapping and etching to ensure surface cleanliness. Thermal analysis of the crystals was performed using a TA Instruments model Q 600 TGA analyzer, recording TGA/DTA/DSC curves from $30^\circ C$ to $1000^\circ C$ in a nitrogen atmosphere at a heating rate of $10^\circ C$. Mechanical behavior studies were conducted using an Omni Tech Vicker micro hardness tester with a light microscope. The flat crystal surface underwent static indentation with loads ranging from 5 mg to 25 mg, and hardness and Mayer's index numbers were compared for analysis.

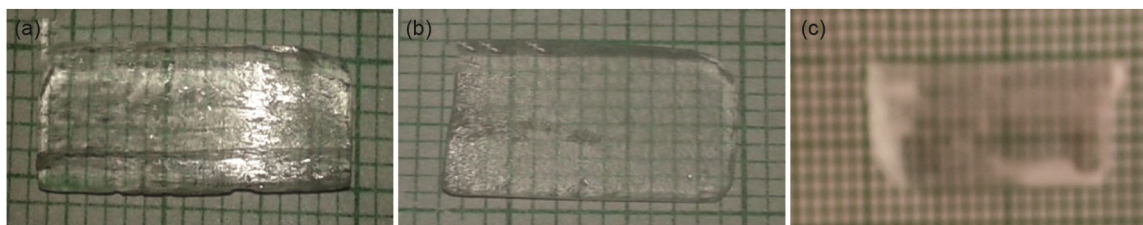


Fig. 1 — a) 1 mol % Mn doped, (b) 2 mol % Mn doped, and (c) 5 mol % Mn doped LOMHCL

4 Results and Discussions

4.1 Powder X-ray Diffraction Analysis

The specimen was crushed into fine powder and then subjected to powder X-ray analysis. The recorded curve for 1 mol %, 2 mol % and 5 mol % MnCl₂ doped LOMHCl crystal are shown in the Fig. 2. The XRD pattern of the doped crystals was found same with only one or two peak having varied intensity. All the peaks were successfully indexed with the help of checkcell software and cell parameters were refined. The refined value for pure LOMHCl crystal was found in well agreement with the literature¹⁴. On deep study of the observed XRD pattern, insignificant small variation in lattices parameters indicates that dopants atom has been incorporated in between the lattice of LOMHCl crystal as reported earlier¹⁴. The presence of no extra peak specifies that no other phase is integrated in the grown crystal due to doping of MnCl₂ doping. The XRD curves were carefully analyzed and full width at half maxima (FWHM) were obtained for each peak conforming to different value of 2θ. Moreover, using Williamson-Hall analysis, we plotted a graph between sin θ and βcos θ and linear fitted. Value of slope of the line is determined from the W-H plot and this gives value of mechanical strain present in the crystal. The value of mechanical strain for 1 mol %, 2 mol % and 5 mol % doped crystals were found 2.95 × 10⁻³, 1.64 × 10⁻³ and 9.79 × 10⁻⁴, respectively. The decrease in the value of mechanical strain indicates the increase in plasticity nature of material or in other

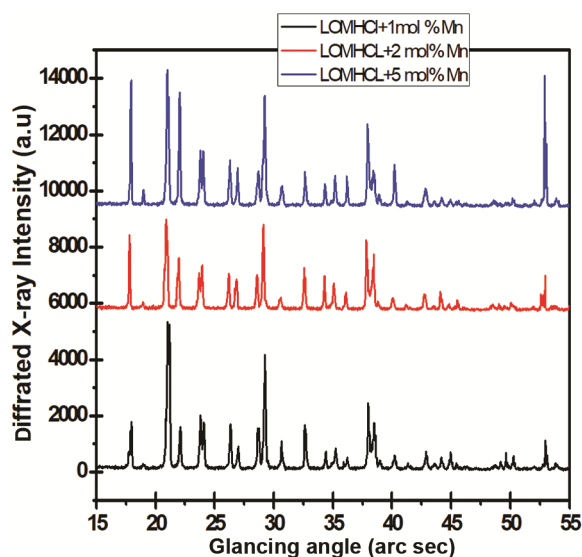


Fig. 2 — Powder XRD curve of 1 mol %, 2 mol % and 5 mol % doped LOMHCl

words we can say hardness increases with increase in dopants concentration.

4.2 HRXRD Analysis

Influence of Mn²⁺ doping on the crystalline perfection of LOMHCl crystal was assessed by employing high-resolution XRD. The HRXRD experiment was conducted as described in the experimental section. All the experimental conditions were kept identical for all doping concentration of the crystal. Very thin transparent crystals were hand lapped and polished before scanning. The rocking /diffraction curves were recorded and full width at half maxima (FWHM) have also been evaluated for each rocking curve of the pure and doped crystals. The recorded curve for pure as well as 1 mol %, 2 mol % and 5 mol % doped LOMHCl single crystals were shown in Figs 3-6, respectively.

The intensity of diffracted x-ray is in arbitrary unit (a.u.) and relative magnitude. All the curves in Figs 3-6 show single peak that confirm the single crystal without any additional phase. The intensity of

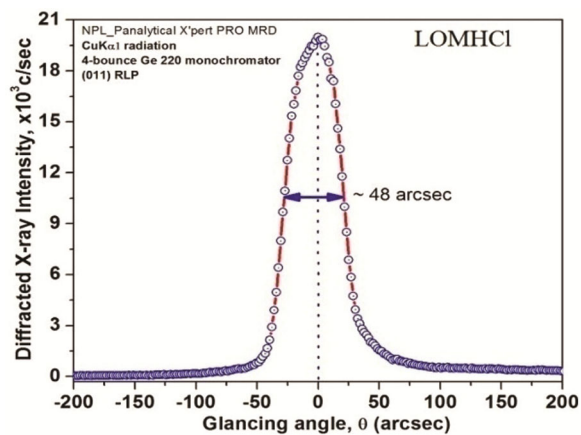


Fig. 3 — Diffraction curve of Pure LOMHCl crystal

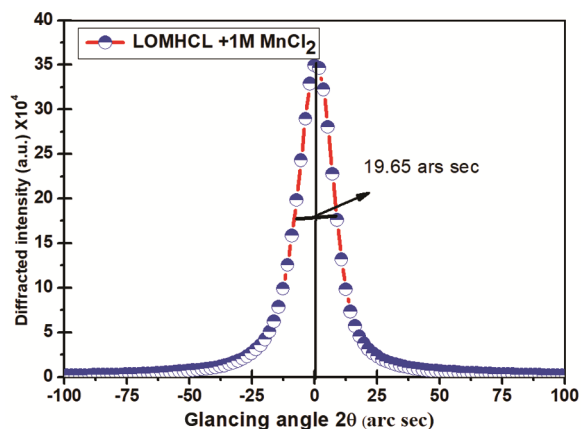


Fig. 4 — Rocking curve of 1 mol % Mn doped LOMHCl crystal

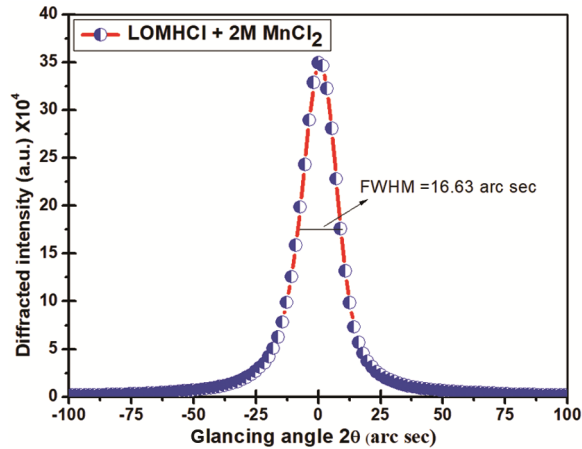


Fig. 5 — Rocking curve of 2 mol% Mn doped

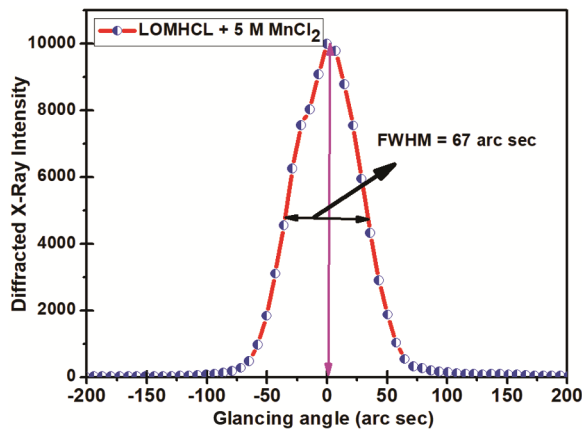


Fig. 6 — Rocking curve of 5 mol % Mn doped LOMHCl crystal
LOMHCl crystal

diffracted X-rays was scattered very less showing that no considerable density of dislocation exists in the crystal. However, on meticulous observation of the rocking curve, some asymmetry is visible on both sides of the peak taken as reference; this is due to point defects and their agglomerates. Large intensity scattering on the negative side of the peak indicates the presence of vacancy type point defects. This can be explained as in the vacancy type point defects the crystal undergoes tensile stress that cause enhancement in lattice parameters around the defect which gives more energy toward -ve side as d and $\sin \theta$ are varying inversely to each other in Bragg's relation. The inverse case is also true, in case of scattered intensity is more on negative side confirms the presence of interstitial type point defects. Detailed report is given in literature¹⁵⁻¹⁷. It is necessary to mention here that small variation in the lattice parameters give scattered intensity near Bragg's peak. Hence small insignificant variation in cell parameters

confirmed that dopants atoms have been incorporated in the crystal lattice.

The rocking curve for 1 mol % MnCl_2 doped L-ornithine monohydrochloride crystal is shown in Fig. 4. The curve contains a single peak with FWHM equal to 19.65 arc sec which is very much less than 48 arc sec recorded for pure LOMHCl crystal. This indicates the enhancement in the crystal perfection. This result is unexpected as the addition of impurities in a crystal improves the crystalline perfection but same was observed in powder XRD. In general case doping of impurity causes defects in crystal resulting in the increase in FWHM of the peak. But experimental findings are opposite to this due to the reason Mn^{2+} ion present in the solution enhances the growth promoting effect. Dopants atoms also restrict the entries of the impurities in crystal growth which is responsible for better crystalline perfection. This type of enhancement in crystal perfection at low doping concentration is due to significant change in growth rate and metastable zone width. Hence, the recorded rocking curve indicate that the dopants atom predominantly occupy vacancy site present in the pure LOMHCl crystal which is revealed by HRXRD. Figure 5 represent the recorded curve for 2 mol % Mn^{2+} doped LOMHCl crystal. The FWHM of the Bragg's peak is 16.63 arc sec which is smaller than pure and 1 mol % doped crystal. This indicates the better crystalline perfection in case of 2 mol %. The FWHM reaches to its minimum value and the defects are minimum in the crystal lattice. This is due the reason that all possible vacancies were filled by dopant atoms as more dopants atoms are available in case of 2 mol %. No additional peak is observed with elucidate that the crystal have the capability of accommodating the dopants atom in its crystal matrix. Similar results were observed in case of KCl doped ADP crystal.

The recorded rocking curve for 5 mol % doped LOMHCl crystal is shown in the Fig. 6. The curve clearly indicates that FWHM has higher than 1 mol % and 2 mol % doped crystal. This enhanced FWHM without any additional peak confirms that crystalline perfection decreases without formation of additional phase at higher doping concentration. This indicates that dopants atoms have incorporated homogeneously in the crystal matrix. This may be due to incorporation of dopants at interstitial position compress the atoms of host material around it. This is because heavy lattices stress induced in crystal which causes the decrease in lattice parameter that leads to

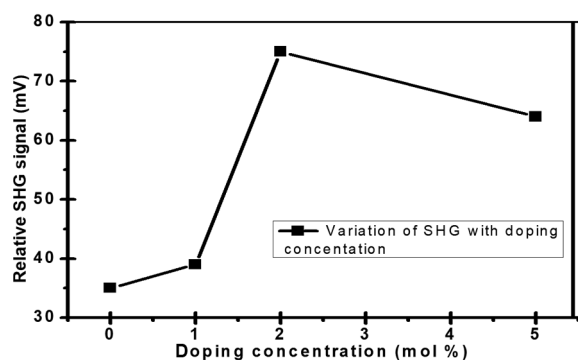


Fig. 7 — Variation of SHG efficiency for varying doping concentration

give more scattered intensity toward negative side. In case of large dopants size, low angle grain boundaries were outlined at very low doping concentration. It is also observed that the heavy stress induced in atoms causes the formation of low angle grain boundaries. Generally, dopants play significant role in enhancing the key properties of crystals and several times with favorable molecular alignment responsible for its SHG efficiency. Here doping do not degraded the crystallinity of the host material due to generation of undesired structural defects such as ‘grain boundaries’.

4.3 Second Harmonic Generation

The Second Harmonic Generation (SHG) efficiency in both pure as well as Mn^{2+} doped LOMHCl crystals was assessed using the Kurtz-powder test. By plotting a graph, correlating doping concentration with output signal, depicted in Fig. 7, the variation in SHG efficiency of LOMHCl crystal due to doping of Mn^{2+} was analyzed. Notably, the graph illustrates an increase in SHG efficiency at 1 mol % and 2 mol % doping, peaking at 2 mol % doping. This finding is consistent with results from HRXRD studies, which elucidate how small concentrations of Mn^{2+} doping eliminates vacancy-type defects within the crystal, thereby reducing the likelihood of SHG photon trapping.

The observed phenomenon significantly enhances SHG efficiency upto moderate doping level, rendering the crystal more effective for Nonlinear Optical (NLO) applications compared to pure LOMHCl. The homogeneous incorporation of moderate concentrations of dopants within the crystal lattice, particularly at interstitial sites, facilitates the exploitation of electronic charge within the lattice environment. However, this incorporation also induces strain in the crystal lattice, intensifying electric-dipole-photon interaction under

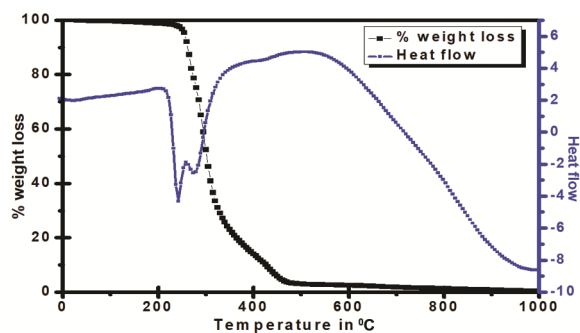


Fig. 8 — TGA/DTA curve of pure LOMHCl crystal

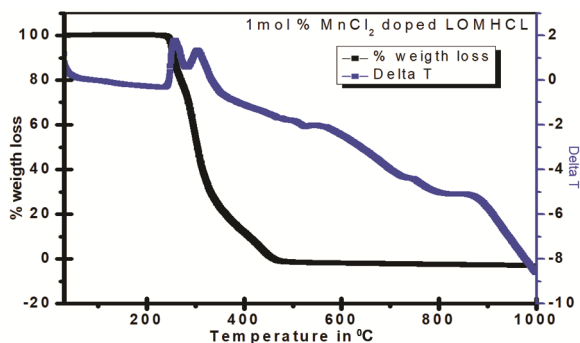


Fig. 9 — TGA/DTA curve of 1 mol % doped LOMHCl crystal

electromagnetic laser radiation. Studies on Nd-strontium niobate crystals have demonstrated that the exploitation of electronic charges within the crystal lattice significantly influences SHG efficiency¹⁸⁻²⁰. However, at 5 mol % doping concentration, a slight decrease in SHG efficiency is observed due to the agglomeration of Mn^{2+} ions, as evidenced by diffraction/rocking curve analysis. This underscores the importance of dopant atom isolation for enhancing SHG efficiency, as clustered dopants typically lose their beneficial properties. These findings are consistent and further validating the results with previous reports on Mn^{2+} doped L-alanine single crystals.

4.4 Thermal Analysis

Thermal behavior of the doped crystal was examined by TGA/DTA analysis. The recorded TGA/DTA curve for pure, 1 mol %, 2 mol % and 5 mol % are shown in Figs 8, 9 and 10, respectively. As in case of pure LOMHCl crystal no weight loss is observed at 100° C indicates the absent of solvent exclusion. Similar behavior is observed after Mn^{2+} doping. Sharpness of peaks in DTA curve shows that crystallinity do not distribute even at high doping concentration. On comparison of these curves one can clearly see that the peak is found slightly shifted toward higher temperature side with the increase in dopant concentration.

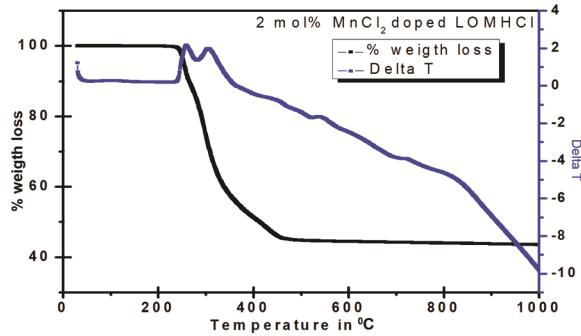
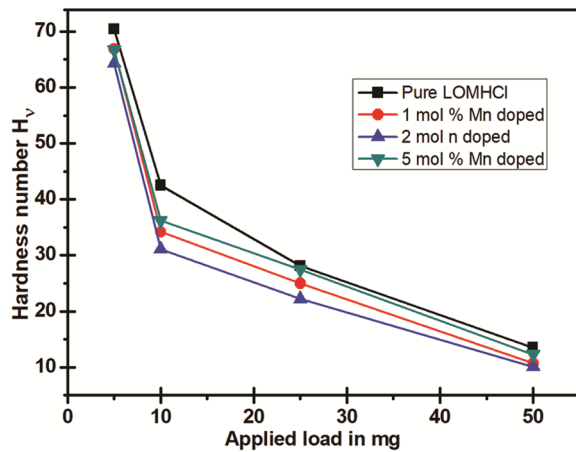


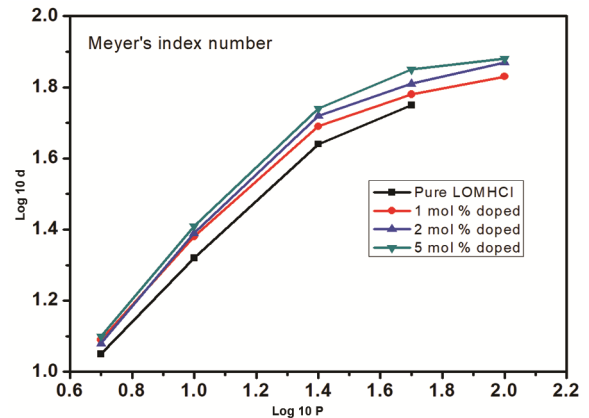
Fig. 10 — TGA/DTA curve of 2 mol % doped LOMHCl crystal

Fig. 11 — Hardness curve for Mn^{2+} doped

The shift observed due to higher concentration may be due to incorporation of Mn^{2+} ion in the lattice of LOMHCl single crystal which is in accordance with the already available reports²¹. The shifting of peak toward higher temperature side indicates that the crystal is confirmed more stable at high temperature. The obtained peaks are found very sharp and the sharpness of the peak indicates better crystallinity of the material²².

4.5 Vicker Microhardness Test

The mechanical behavior of the doped crystals was examined by subjecting the crystal with both the surfaces flat to Vicker microhardness tester as noted in experimental section. Indentation was measured by applying load from 5 gm to 75 gm for 10 s. Some cracks could be easily seen through optical microscope attached with the instrument at moderate value of applied loads. Then hardness number is plotted against the applied load as shown in the Fig. 11. From this Fig. 11, it is clear that for all doping concentration micro-hardness number decreases with increase in load values. But at a particular value of applied load, hardness number

Fig. 12 — Meyer's index curve of Mn^{2+} doped

increases with the increase in doping concentration up to a moderate level and slightly decreases at higher doping concentration.

LOMHCl crystal LOMHCl crystal

Further, using the Meyer's law, $P = a \cdot d^n$, here P denotes the load applied on the surface of crystal, d represents average of diagonal length and n represent the Meyer's index number.

$$P = a \cdot d^n$$

Taking log on both sides, we get $\log P = n \cdot \log d$. Meyer's index number is calculated from the plot between $\log P$ and $\log d$ as shown in the figure. The slope of the above plot is the value of Meyer's index number and it is obtained 1.06, 1.04, 1.04 and 1.03 for undoped and doped with 1 mol %, 2 mol % and 5 mol % of Mn in LOMHCl single crystals respectively. Onitsch²³ reported that value of Meyer's index number lying between $1.0 < n < 1.6$ that represents the hard material and for $n > 1.6$ is for soft material^{23,24}. Above results confirm that mechanical hardness increases with increase in doping concentration and hence doped material is found more mechanically stable and hard as compared to undoped LOMHCl.

5 Conclusion

Single crystals of 1 mol %, 2 mol % and 5 mol % doped LOMHCl were successfully grown by SEST method at ordinary temperature. The unit cell parameters of Mn^{2+} doped crystals were also calculated with the help of checkcell software using the powder XRD data. The present investigation reveals that LOMHCl is found highly capable for accommodating Mn^{2+} ions at the vacant site of the lattice without forming any structural grain boundaries. Crystalline

perfection of the grown crystals was assessed using high-resolution XRD technique and found fairly better for moderate doping concentration. However, high concentration of dopants leads to reduction of laser properties of LOMHCl single crystal. The UV-Vis spectroscopy results confirmed high transmission in entire visible and near infra-red range for low and moderate doping concentration but a small reduction of transmission for higher doping concentration (5 mol %) has been observed. Thermal analysis of the grown crystal confirmed the doped crystals are found more thermally stable as compared to pure LOMHCl. Moreover, Vicker micro-hardness test indicates the increase in mechanical strength in terms of mechanical stability. Hence, it is concluded that, these enhanced SHG efficiency, crystalline perfection and optical transparency due to doping of Mn^{2+} ion increases the suitability of crystal for laser application.

References

- 1 Kang H, Yang C X, Mu G G & Wu Z K, *Opt Letters*, 15 (1990) 637.
- 2 Natrajan S, Martin Britto Dhas S A & Ramachanderan E, *Cryst Growth Des*, 6 (2006) 137.
- 3 Yoshida H, Futija H, Nakatsuka M, Yoshimura M, Sasaki T, Kamimura T & Yoshida K, *J Appl Phys*, 45 (2006) 137.
- 4 Shkir M, Riscob B & Bhagavannarayan G, *Solid State Sci*, 14 (2012) 773.
- 5 Ashwell G J, Jefferies G, Hamilton D G, Lynch D E, Robert M P S, Behra G S & Brown C R, *Nature*, 375 (1995) 385.
- 6 Lim D, Downer M C, Ekerdt J G, Arzate N, Manddoza B S, Gavrilenko V I & Wu R Q, *Phys Rev Letters*, 84 (2000) 3406.
- 7 Ramirez M O, Jaque D, Bausa L E, sole Garci J & Kaminskii A A, *Phys Rev Letters*, 84 (2005) 267401.
- 8 Takeda K, Arata Y & Fujiwara S, *J Chem Phys*, 53 (1970) 854.
- 9 Winkler E, Fainstein A, Etchegoin P & Fainstein C, *Phys Rev B*, 61 (2000) 15756
- 10 Bhagavannarayana G & Kushwaha S K, *J Appl Cryst*, 43 (2010) 154.
- 11 Kushwaha S K, Rathee S P, Maurya K K & Bhagavannarayan G, *J Cryst Growth*, 328(1) (2011) 81.
- 12 Kumar B S, Jagadeesh M R & Kumar H M S, *J Mater Sci: Mater Electron*, 33 (2022) 26706.
- 13 Hiti A, Nekkach F, Boutahar A, Moubah R, Lemziouka H & Hlil E K, *Opt Mater*, 143 (2023) 114161.
- 14 Krishna A, Vijayan N, Riscob B, Gour B S, Haranath D, Philip J, Verma S, Jayalakshmy M S, Bhagavannarayana G & Halder S K, *Appl Phys A*, 114 (4) (2014) 1257.
- 15 Rathee S P, Singh D & Ahlawat, *Optik*, 136 (2017) 249.
- 16 Davey R J & Mullin J W, 23 (1974) 89.
- 17 Bhagavannarayan G, Parthiban S & Meenakshisunderam S, *J Cryst Growth Growth Des*, 8 (2008) 446.
- 18 Bhagavannarayana G, Kushwaha S K, Parthiban S, Ajitha G & Meenakshisunderam S, *J Cryst Growth*, 310 (2008) 2575.
- 19 Furulkawa Y, Yokotani A, Sasaki T, Yoshida H, Yoshida K, Nitanda F & Satco M, *J Appl Phys*, 69 (1991) 3372.
- 20 Ramo D M, Gavartin J L & Bersuker G, *Phys Rev B*, 75 (2007) 205336.
- 21 Buse K, Adibi A & Psaltis D, *Nature*, 393 (1998) 665.
- 22 Bright K C & Freeda T H, *J Therm anal Calorim*, 112 (2013) 1185.
- 23 Muthu K, Bhagavannarayana G, Chandrasekaran C, Parthiban S, Meenakshisundaram S P & Mojumdar S C, *J Therm Anal Calorim*, 100 (2010) 793.
- 24 Onitsch E M, *Milroscope*, 95 (1968) 3798.